Chapter 4

A Fourth Order Accurate Numerical Method for Nonlinear Time Fractional Reaction–Diffusion Equation on a Bounded Domain

This chapter deals with solving nonlinear Caputo time fractional reaction–diffusion equation. The time fractional derivative is approximated using time stepping cubic interpolating polynomial and spatial derivatives are approximated by compact difference scheme. A rigorous analysis of stability, solvability and convergence of the scheme is studied. Numerical examples are provided to support theoretical findings.

4.1 Introduction

Consider the following nonlinear Caputo time fractional reaction–diffusion equation,

$$\begin{cases} {}_0^C D_t^\alpha u(x,t) = K\frac{\partial^2 u}{\partial x^2} + f(u) + F(x,t), \qquad (x,t) \in \Omega \times (0,T], \\ u(x,0) = u_0(x), \text{ on } \Omega \\ u(a,t) = u_a(t), \\ u(b,t) = u_b(t), \text{ on } [0,T] \end{cases} \tag{4.1}$$

where $\bar{\Omega} = [a,b]$. $D > 0$, is the diffusion coefficient, $f(u)$ is the reaction term which satisfies the Lipschitz condition,

$$|f(u(x_1,t)) - f(u(x_2,t))| \leq L|u(x_1,t) - u(x_2,t)|, \forall x_1, x_2 \in \Omega, \tag{4.2}$$

with L as a positive Lipschitz constant and $F(x,t)$, $u_0(x)$, $u_a(t)$, $u_b(t)$ are sufficiently smooth known functions. The fractional exponent $\alpha \in (0,1)$ and the fractional derivative is defined in the Caputo sense for sufficiently regular function $u(x,t)$.

In the present chapter, a high order numerical scheme is proposed to solve the nonlinear Caputo time fractional reaction–diffusion equation (4.1). We use the cubic approximation formula for Caputo time fractional derivative discussed by Cao et al. [104] and compact finite difference approximation for spatial derivative. Further, the Newton–Raphson iterative algorithm is adopted to solve the obtained fully discrete nonlinear system. The solvability, stability analysis and convergence analysis are proved rigorously for the proposed scheme. The stability and convergence are achieved using von Neumann stability analysis and Matrix analysis respectively. The difference scheme is proved to have $(4-\alpha)$th order accuracy in the temporal direction and 4th order accuracy in the spatial direction, which as to the authors'

knowledge is the highest order accuracy in the literature. The rest of the chapter is organized as follows: in Section 4.2 some basic notations and lemmas are discussed and we construct the compact finite difference scheme in Section 4.3. The unique solvability, stability and convergence of the scheme are proved in the Section 4.4. In Section 4.5, some numerical examples are provided to show the efficiency of the scheme and to validate our theoretical findings. Finally, some concluding remarks are drawn in the Section 4.6.

4.2 Notations and Preliminary Lemmas

In this subsection, we study some essential and prerequisite notations and lemmas. Let $\tau = \frac{T}{N}$, and $h = \frac{b-a}{M}$, are the temporal and spatial step sizes respectively. Let $\bar{\Omega}_\tau = \{t_n = n\tau : 0 \leq n \leq N\}$, and $\bar{\Omega}_h = \{x_i = a + ih : 0 \leq i \leq M\}$ and define $\Omega_{h\tau} = \bar{\Omega}_h \times \bar{\Omega}_\tau$. For the grid function space $\omega_h = \{\omega_i : 1 \leq i \leq M-1\}$, defined on $\bar{\Omega}_h$, we define for any grid function $\omega_i \in \omega_h$,

$x_{i+\frac{1}{2}} = \frac{1}{2}(x_i + x_{i+1})$, $\delta_x w_{i-\frac{1}{2}} = \frac{1}{h}(w_i - w_{i-1})$, $\delta_x^2 w_i = \frac{1}{h}(\delta_x w_{i+\frac{1}{2}} - \delta_x w_{i-\frac{1}{2}})$.

The compact difference operator is defined as [105],

$$\mathcal{H}_x w_i = \begin{cases} \frac{1}{12}(w_{i+1} + 10w_i + w_{i-1}) = (1 + \frac{h^2}{12}\delta_x^2)w_i, & 1 \leq i \leq M-1 \\ w_i, & i = 0 \text{ or } M \end{cases}. \tag{4.3}$$

Let $\omega_\tau = \{v^n : 1 \leq n \leq N\}$, be any grid function space defined on $\bar{\Omega}_\tau$. For any $v^n \in \bar{\Omega}_\tau$, we have [104]

$$ {}_0^C D_t^\alpha v^n = \frac{\tau^{-\alpha}}{\Gamma(2-\alpha)} \sum_{j=0}^{n} \psi_j v^{n-j} + R^n, \tag{4.4}$$

where discretization coefficients for various values of n are given as:

For $n = 1$

$$\begin{cases} \psi_0 = \vartheta_0, \\ \psi_1 = -\vartheta_0. \end{cases}$$

For $n = 2$

$$\begin{cases} \psi_0 = \vartheta_0 + \varphi_0, \\ \psi_1 = \vartheta_1 - \vartheta_0 - 2\varphi_0, \\ \psi_2 = \varphi_0 - \vartheta_1. \end{cases}$$

For $n = 3$

$$\begin{cases} \psi_0 = \kappa_{1,0}, \\ \psi_1 = \kappa_{2,0} + \vartheta_1 + \varphi_1, \\ \psi_2 = \kappa_{3,0} + \vartheta_2 - \vartheta_1 - 2\varphi_1, \\ \psi_3 = \kappa_{4,0} - \vartheta_2 + \varphi_1. \end{cases}$$

For $n = 4$

$$\begin{cases} \psi_0 = \kappa_{1,0}, \\ \psi_1 = \kappa_{1,1} + \kappa_{2,0}, \\ \psi_2 = \kappa_{2,1} + \kappa_{3,0} + \vartheta_2 + \varphi_2, \\ \psi_3 = \kappa_{3,1} + \kappa_{4,0} + \vartheta_3 - \vartheta_2 - 2\varphi_2, \\ \psi_4 = \kappa_{4,1} - \vartheta_3 + \varphi_2. \end{cases}$$

For $n = 5$

$$\begin{cases} \psi_0 = \kappa_{1,0}, \\ \psi_1 = \kappa_{1,1} + \kappa_{2,0}, \\ \psi_2 = \kappa_{1,2} + \kappa_{2,1} + \kappa_{3,0}, \\ \psi_3 = \kappa_{2,2} + \kappa_{3,1} + \kappa_{4,0} + \vartheta_3 + \varphi_3, \\ \psi_4 = \kappa_{3,2} + \kappa_{4,1} + \vartheta_4 - \vartheta_3 - 2\varphi_3, \\ \psi_5 = \kappa_{4,2} - \vartheta_4 + \varphi_3. \end{cases}$$

For $n \geq 6$

$$\begin{cases} \psi_0 = \kappa_{1,0}, \\ \psi_1 = \kappa_{1,1} + \kappa_{2,0}, \\ \psi_2 = \kappa_{1,2} + \kappa_{2,1} + \kappa_{3,0}, \\ \psi_s = \kappa_{1,s} + \kappa_{2,s-1} + \kappa_{3,s-2} + \kappa_{4,s-3}, 3 \leq s \leq n-3, \\ \psi_{n-2} = \vartheta_{n-2} + \varphi_{n-2} + \kappa_{2,n-3} + \kappa_{3,n-4} + \kappa_{4,n-5}, \\ \psi_{n-1} = \kappa_{3,n-3} + \kappa_{4,n-4} + \vartheta_{n-1} - \vartheta_{n-2} - 2\varphi_{n-2}, \\ \psi_n = \kappa_{4,n-3} - \vartheta_{n-1} + \varphi_{n-2}, \end{cases}$$

also,

$$\vartheta_w = (w+1)^{(1-\alpha)} - w^{(1-\alpha)}, \tag{4.5}$$

$$\varphi_w = \frac{(w+1)^{(2-\alpha)} - w^{(2-\alpha)}}{(2-\alpha)} - \frac{(w+1)^{(1-\alpha)} + w^{(1-\alpha)}}{2}, \tag{4.6}$$

$$\begin{aligned} \kappa_{1,w} = {} & \frac{1}{6}[2(w+1)^{(1-\alpha)} - 11w^{(1-\alpha)}] - \frac{1}{(2-\alpha)}[2w^{(2-\alpha)} - (w+1)^{(2-\alpha)}] \\ & - \frac{1}{(2-\alpha)(3-\alpha)}[w^{(3-\alpha)} - (w+1)^{(3-\alpha)}], \end{aligned} \tag{4.7}$$

$$\begin{aligned} \kappa_{2,w} = {} & \frac{1}{2}[(w+1)^{(1-\alpha)} + 6w^{(1-\alpha)}] + \frac{1}{(2-\alpha)}[5w^{(2-\alpha)} - 2(w+1)^{(2-\alpha)}] \\ & + \frac{3}{(2-\alpha)(3-\alpha)}[w^{(3-\alpha)} - (w+1)^{(3-\alpha)}], \end{aligned} \tag{4.8}$$

$$\kappa_{3,w} = -\frac{1}{2}[2(w+1)^{(1-\alpha)} + 3w^{(1-\alpha)}] - \frac{1}{(2-\alpha)}[4w^{(2-\alpha)} - (w+1)^{(2-\alpha)}]$$
$$- \frac{3}{(2-\alpha)(3-\alpha)}[w^{(3-\alpha)} - (w+1)^{(3-\alpha)}], \tag{4.9}$$
$$\kappa_{4,w} = \frac{1}{6}[(w+1)^{(1-\alpha)} + 2w^{(1-\alpha)}] - \frac{1}{(2-\alpha)}w^{(2-\alpha)}$$
$$+ \frac{1}{(2-\alpha)(3-\alpha)}[w^{(3-\alpha)} - (w+1)^{(3-\alpha)}]. \tag{4.10}$$

Lemma 4.2.1. [106] Let $\xi(s) = (1-s)^3(5-3(1-s)^2)$, and let function $\phi(x) \in C^6[0, L]$, then for $1 \leq i \leq M-1$,

$$\mathcal{H}_x\phi''(x_i) = \delta_x^2\phi(x_i) + \frac{h^4}{360}\int_0^1 [\phi^{(6)}(x_i - sh) + \phi^{(6)}(x_i + sh)]\xi(s)ds. \tag{4.11}$$

Lemma 4.2.2. [104] Let $\phi(t) \in C^4[0, t]$ then for any $0 < \alpha < 1$, the truncation errors $|R^n|$ satisfies the following,

1. $|R^1| \leq C_1 \max_{t_0 \leq t \leq t_1} |f''(t)|\tau^{2-\alpha},\ C_1 > 0,\ n = 1,$
2. $|R^2| \leq C_2 \max_{t_0 \leq t \leq t_2} |f'''(t)|\tau^{3-\alpha},\ C_2 > 0,\ n = 2,$
3. $|R^n| \leq \frac{1}{\Gamma(1-\alpha)}\{\frac{2\alpha}{3}\max_{t_0 \leq t \leq t_2} |f'''(t)|(t_n - t_2)^{-\alpha-1}\tau^4$
   $+ [\frac{1}{12} + \frac{3\alpha^2}{2(1-\alpha)(2-\alpha)}]\max_{t_0 \leq t \leq t_n} |f^4(t)|\tau^{4-\alpha}\},\ n \geq 3.$

Further, quoting the results from [104] we discuss few properties of the discretization coefficients obtained in construction of the scheme.

Lemma 4.2.3. [104] For any $0 < \alpha < 1$ the discretization coefficients satisfies the following properties,

1. If $n = 1$ is fixed then $\psi_1 = -\psi_0$.
2. If $n = 2$ is fixed and $\alpha \in (0, \bar{\alpha})$, then $|\psi_1| + |\psi_2| = |\psi_0|$, where $\bar{\alpha} \approx 0.67$ is the unique solution of equation $\frac{\alpha}{2(2-\alpha)} - 2^{1-\alpha} + 1 = 0$ for $\alpha \in (0, 1)$.

Lemma 4.2.4. [104] For $n \geq 3$ and $0 < \alpha < 1$ following properties hold for the discretization coefficients ψ_j

1. $\psi_0 = \frac{1}{3} + \frac{1}{(2-\alpha)} + \frac{1}{(2-\alpha)(3-\alpha)} \in (1, \frac{11}{6})$,
2. $\psi_2 > 0$,
3. $\psi_j < 0, j \geq 1, j \neq 2$,
4. $\psi_2 - \psi_1 - \psi_3 \leq \psi_0$, for $\alpha \in (0, \hat{\alpha})$, such that $\hat{\alpha}$ can be uniquely determined by the equation, $\kappa_{1,2} + \kappa_{2,1} + \kappa_{3,0} - \kappa_{1,1} - \kappa_{2,0} - \kappa_{4,0} - \kappa_{3,1} - \kappa_{2,2} - \kappa_{1,3} - \kappa_{1,0} = 0$, for $\alpha \in (0, 1)$,
5. $\psi_2 - \psi_1 - \psi_3 - \psi_4 \leq \psi_0$, for $\alpha \in (0, \hat{\hat{\alpha}})$, such that, $\hat{\hat{\alpha}}$ can be uniquely determined by the equation, $\kappa_{1,2} + \kappa_{2,1} + \kappa_{3,0} - \kappa_{1,1} - \kappa_{2,0} - \kappa_{1,3} - \kappa_{2,2} - \kappa_{3,1} - \kappa_{4,0} - \kappa_{1,4} - \kappa_{2,3} - \kappa_{3,2} - \kappa_{4,1} - \kappa_{1,0} = 0$, for $\alpha \in (0, 1)$,
6. $\sum_{j=0}^{n} \psi_j = 0$.

4.3 Construction of the Scheme

Now, we construct the compact finite difference scheme for the considered equation (4.1) at the node point (x_i, t_n),

$$ {}_0^C D_t^\alpha u(x_i, t_n) = K \frac{\partial^2 u(x_i, t_n)}{\partial x^2} + f(u(x_i, t_n)) + F(x_i, t_n). $$

Let us assume the grid functions, $u(x_i, t_n) = u_i^n$, and $F(x_i, t_n) = F_i^n$, for $0 \leq i \leq M$, and $0 \leq n \leq N$. So from (4.4) and Lemma 4.2.2, we have

$$ \frac{\tau^{-\alpha}}{\Gamma(2-\alpha)} \sum_{j=0}^{n} \psi_j u_i^{n-j} = K \frac{\partial^2 u_i^n}{\partial x^2} + f(u_i^n) + F_i^n + \mathcal{O}(\tau^{4-\alpha}). \tag{4.12} $$

Applying compact difference operator (4.3) on both sides of (4.12) and using Lemma 4.2.1, we have

$$\sum_{j=0}^{n}\psi_j\mathcal{H}_x u_i^{n-j} = K\delta_x^2 u_i^n + \tau^\alpha\Gamma(2-\alpha)\mathcal{H}_x(f(u_i^n)+F_i^n) + R_i^n,$$
$$\sum_{j=0}^{n}\frac{\psi_j}{12}(u_{i+1}^{n-j}+10u_i^{n-j}+u_{i-1}^{n-j}) = \frac{\tau^\alpha\Gamma(2-\alpha)K}{h^2}(u_{i+1}^n-2u_i^n+u_{i-1}^n)$$
$$+\frac{\tau^\alpha\Gamma(2-\alpha)}{12}\big((f(u_{i+1}^n)+10f(u_i^n)+f(u_{i-1}^n))$$
$$+(F_{i+1}^n+10F_i^n+F_{i-1}^n)\big)+R_i^n. \tag{4.13}$$

where $|R_i^n| \le C(\tau^{4-\alpha}+h^4)$, $1 \le i \le M-1$, $3 \le n \le N$, for constant $C > 0$. Denoting $\mu = \frac{K\tau^\alpha\Gamma(2-\alpha)}{h^2}$ and omitting the small term R_i^n in the above relation we obtain the following form of the proposed scheme,

$$\mu(U_{i+1}^n-2U_i^n+U_{i-1}^n)-\frac{\psi_0}{12}(U_{i+1}^n+10U_i^n+U_{i-1}^n)+\frac{\tau^\alpha\Gamma(2-\alpha)}{12}(f(U_{i+1}^n)$$
$$+10f(U_i^n)+f(U_{i-1}^n)) = \sum_{j=1}^{n}\frac{\psi_j}{12}(U_{i+1}^{n-j}+10U_i^{n-j}+U_{i-1}^{n-j})$$
$$-\frac{\tau^\alpha\Gamma(2-\alpha)}{12}(F_{i+1}^n+10F_i^n+F_{i-1}^n). \tag{4.14}$$

Now, matrix form of (4.14) can be obtained as,

$$A^nU^n+\tau^\alpha\Gamma(2-\alpha)A_2f(U^n) = \sum_{j=1}^{n}\psi_jA_2U^{n-j}-\tau^\alpha\Gamma(2-\alpha)A_2F^n+B^n, \tag{4.15}$$

where

$$A^n = [\mu A_1-\psi_0A_2],$$
$$U^n = [U_1^n, U_2^n, \cdots, U_{M-1}^n]^T,$$
$$B^n = \mu_0^nI_1+\mu_M^nI_n,$$

$$\mu_0^n = \sum_{j=0}^{n} \psi_j U_a^{n-j} - \mu U_a^n - \frac{\tau^\alpha \Gamma(2-\alpha)}{12}(f(U_a^n) + F_0^n),$$

$$\mu_M^n = \sum_{j=0}^{n} \psi_j U_b^{n-j} - \mu U_b^n - \frac{\tau^\alpha \Gamma(2-\alpha)}{12}(f(U_b^n) + F_M^n),$$

$$I_1 = [1, 0, \cdots, 0]^T, \quad I_M = [0, \cdots 0, 1]^T,$$

$$F^n = [F_1^n, F_2^n, \cdots, F_{M-1}^n]^T,$$

$$A_2 = \frac{1}{12}\begin{bmatrix} 10 & 1 & & & \\ 1 & 10 & 1 & & \\ & \ddots & \ddots & \ddots & \\ & & \ddots & \ddots & 1 \\ & & & 1 & 10 \end{bmatrix}, \quad A_1 = \begin{bmatrix} -2 & 1 & & & \\ 1 & -2 & 1 & & \\ & \ddots & \ddots & \ddots & \\ & & \ddots & \ddots & 1 \\ & & & 1 & -2 \end{bmatrix}.$$

4.3.1 An Iterative Algorithm for the Nonlinear Reaction Term

Eq. (4.15) becomes a system of nonlinear algebraic equations when $f(u)$ is a non linear function of u. A nonlinear solver is required to solve such nonlinear system of equations. Due to comparatively fast rate of convergence and easy implementation, we use the Newton–Raphson's iterative algorithm for solving the nonlinear system of equation (4.15). To apply the Newton's method, we obtain the following iterative form of (4.15),

$$A^n U^{[n,s+1]} + \tau^\alpha \Gamma(2-\alpha) A_2 f(U^{[n,s+1]}) = \sum_{j=1}^{n} \psi_j A_2 U^{n-j} - \tau^\alpha \Gamma(2-\alpha) A_2 F^n + B^n, \ 1 \le n \le N, s \ge 0. \tag{4.16}$$

Applying the Newton's method to term $f(U^{[n,s+1]})$, we have

$$f(U^{[n,s+1]}) = f(U^{[n,s]}) + (U^{[n,s+1]} - U^{[n,s]})f'(U^{[n,s]}). \tag{4.17}$$

Substituting (4.17) into (4.16) we obtain the following Newton's iterative formula,

$$\begin{aligned}(A^n + \tau^\alpha \Gamma(2-\alpha)A_2 f'(U^{[n,s]}))U^{[n,s+1]} = \tau^\alpha \Gamma(2-\alpha)A_2(f'(U^{[n,s]})U^{[n,s]} - f(U^{[n,s]})) \\ + \sum_{j=1}^{n} \psi_j A_2 U^{n-j} - \tau^\alpha \Gamma(2-\alpha)A_2 F^n + B^n,\end{aligned} \tag{4.18}$$

where $U^{[n,s]}$ is the value of sth step iteration at the nth time level.

4.4 Numerical Analysis

In this section, we will prove the solvability, numerical stability and convergence for the finite difference scheme (4.14).

Lemma 4.4.1. The eigenvalues of the matrices A_2 and A_1 are $\lambda^i_{A_2} = 1 - \frac{1}{3}\sin^2\left(\frac{i\pi}{2M}\right), i = 1, 2, \cdots, M-1$ and $\lambda^i_{A_1} = -4\sin^2(\frac{i\pi}{2M}), i = 1, 2, \cdots, M-1$ respectively.

Proof. The eigenvalues of a tridiagonal matrix, of the form tri[Z X Y] are given as [98, pg.154],

$$\lambda_i = X + 2Y\left(\frac{Z}{Y}\right)^{\frac{1}{2}} \cos\left(\frac{i\pi}{N}\right), i = 1, 2, \cdots, M-1.$$

So the eigenvalues of the matrix A_2 will be,

$$\lambda^i_{A_2} = \frac{1}{12}\left[10 + 2\cos\left(\frac{i\pi}{M}\right)\right]$$

$$=1-\frac{1}{3}\sin^2\left(\frac{i\pi}{2M}\right),\ i=1,2,\cdots,M-1.$$

Similarly, the eigenvalues of A_1 are obtained as

$$\begin{aligned}\lambda^i_{A_1} &= -2+2\cos\left(\frac{i\pi}{M}\right)\\ &= -4\sin^2\left(\frac{i\pi}{2M}\right),\ i=1,2,\cdots,M-1.\end{aligned}$$

□

From Lemma 4.4.1, we conclude that the eigenvalues of the matrix A^n will be

$$\begin{aligned}\lambda^i_{A^n} &= \mu\left(-4\sin^2\left(\frac{i\pi}{2M}\right)\right)-\psi_0\left(1-\frac{1}{3}\sin^2\left(\frac{i\pi}{2M}\right)\right),\\ &= \left(\frac{\psi_0}{3}-4\mu\right)\sin^2\left(\frac{i\pi}{2M}\right)-\psi_0,\end{aligned}\tag{4.19}$$

which is never zero, hence the matrix A^n is invertible, which implies unique solvability of the finite difference scheme (4.15) when $f(u)=0$.

4.4.1 Stability Analysis

Theorem 4.4.1. Finite difference scheme (4.15) is numerically stable for $0<\alpha<1$.

Proof. Here, we study the numerical stability analysis of the proposed scheme (4.13). The numerical stability is established if corresponding to any small perturbation term introduced in the system there is a small perturbation in the numerical solution. Consider $\hat{U}$ as the solution of the perturbed equation obtained introducing the perturbation term τ_i^n. We will examine how the perturbation $\tau_i^n = U_i^n - \hat{U}_i^n$ propagates with time. From (4.13) we see that the perturbation term τ_i^n satisfies

the following system

$$\begin{aligned}
&\mu(\tau_{i+1}^n - 2\tau_i^n + \tau_{i-1}^n) - \frac{\psi_0}{12}(\tau_{i+1}^n + 10\tau_i^n + \tau_{i-1}^n) = \sum_{j=1}^{n} \frac{\psi_j}{12}(\tau_{i+1}^{n-j} + 10\tau_i^{n-j} + \tau_{i-1}^{n-j}) \\
&\quad - \frac{\tau^\alpha \Gamma(2-\alpha)}{12}\Big((f(U_{i+1}^n) - f(\tilde{U}_{i+1}^n)) + 10(f(U_i^n) - f(\tilde{U}_i^n)) + (f(U_{i-1}^n) - f(\tilde{U}_{i-1}^n))\Big) \\
&\leq \sum_{j=1}^{n} \frac{\psi_j}{12}(\tau_{i+1}^{n-j} + 10\tau_i^{n-j} + \tau_{i-1}^{n-j}) - \frac{\tau^\alpha \Gamma(2-\alpha)L}{12}(\tau_{i+1}^n + 10\tau_i^n + \tau_{i-1}^n),
\end{aligned}$$

so we have

$$\begin{aligned}
\mu(\tau_{i+1}^n - 2\tau_i^n + \tau_{i-1}^n) + \frac{\tau^\alpha \Gamma(2-\alpha)L - \psi_0}{12}(\tau_{i+1}^n + 10\tau_i^n + \tau_{i-1}^n) \\
\leq \sum_{j=1}^{n} \frac{\psi_j}{12}(\tau_{i+1}^{n-j} + 10\tau_i^{n-j} + \tau_{i-1}^{n-j}).
\end{aligned} \tag{4.20}$$

To apply the von Neumann stability analysis, we assume that

$$\tau_i^n = \xi^n e^{I\omega i h}, \tag{4.21}$$

where ω is the wave number and $I = \sqrt{-1}$. From (4.20) and (4.21), we have

$$\begin{aligned}
\xi^n \leq & \frac{(1 - \frac{1}{3}\sin^2(\frac{\omega h}{2}))}{-4\mu \sin^2(\frac{\omega h}{2}) - (\psi_0 - \tau^\alpha \Gamma(2-\alpha)L)(1 - \frac{1}{3}\sin^2(\frac{\omega h}{2}))} \sum_{j=1}^{n} \psi_j \xi^{n-j}, \\
|\xi^n| \leq & \frac{|(1 - \frac{1}{3}\sin^2(\frac{\omega h}{2}))|}{|4\mu \sin^2(\frac{\omega h}{2}) + (\psi_0 - \tau^\alpha \Gamma(2-\alpha)L)(1 - \frac{1}{3}\sin^2(\frac{\omega h}{2}))|} \sum_{j=1}^{n} |\psi_j||\xi^{n-j}|.
\end{aligned} \tag{4.22}$$

By taking h sufficiently small we can make the term $4\mu \sin^2(\frac{\omega h}{2})$ large enough, where $\mu = \frac{K\tau^\alpha \Gamma(2-\alpha)}{h^2}$, so that $|4\mu \sin^2(\frac{\omega h}{2}) + (\psi_0 - \tau^\alpha \Gamma(2-\alpha)L)(1 - \frac{1}{3}\sin^2(\frac{\omega h}{2}))| \geq |1 - \frac{1}{3}\sin^2(\frac{\omega h}{2})|$. This condition can always be made true by choosing appropriate h and τ so we have

$$\frac{|1 - \frac{1}{3}\sin^2(\frac{\omega h}{2})|}{|4\mu \sin^2(\frac{\omega h}{2}) + (\psi_0 - \tau^\alpha \Gamma(2-\alpha)L)(1 - \frac{1}{3}\sin^2(\frac{\omega h}{2}))|} \leq 1. \tag{4.23}$$

So, from (4.22) and (4.23) we obtain

$$|\xi^n| \leq \sum_{j=1}^{n} |\psi_j||\xi^{n-j}|. \tag{4.24}$$

Now, we prove that $|\xi^n| \leq |\xi^0|$, for all n using the idea of mathematical induction. For $n = 1$, $|\xi^1| \leq |\psi_1||\xi^0|$, by the property 1 of Lemma 4.2.3, and using the value of ψ_0, for $n = 1$, we have, $|\xi^1| \leq |\xi^0|$. Again let us assume that,

$$|\xi^n| \leq |\xi^0|, \ n = 2, 3, \cdots, n-1. \tag{4.25}$$

Using (4.25) in (4.24) and by property 6 of Lemma 4.2.4, we have

$$\begin{aligned} |\xi^n| &\leq \sum_{j=1}^{n} |\psi_j||\xi^0| \\ &= (\psi_0 + 2\psi_2)|\xi^0| \\ &\leq C|\xi^0|, \end{aligned}$$

where $C = \psi_0 + 2\psi_2$. Hence (4.25) is true for all n, which implies that perturbation is bounded with each marching step in time. This proves the stability of the proposed finite difference scheme (4.13). □

4.4.2 Convergence Analysis

Theorem 4.4.2. The compact difference scheme (4.15) is $(4-\alpha)$th order accurate in time and 4th order accurate in space, i.e.,

$$\|U^n - u^n\|_2 \leq \tilde{C}(\tau^{4-\alpha}, h^4), \ n \geq 3. \tag{4.26}$$

Proof. We prove theorem 4.4.2 using matrix analysis [107]. Let us introduce the notation $E^n = U^n - u^n$, subtracting (4.13) and (4.14), in their matrix form we obtain

$$\begin{aligned}
A^n(U^n - u^n) &= -\tau^\alpha\Gamma(2-\alpha)A_2(f(U^n) - f(u^n)) + \sum_{j=1}^{n}\psi_j A_2(U^{n-j} - u^{n-j}) + R^n,\\
A^n(U^n - u^n) &\leq -\tau^\alpha\Gamma(2-\alpha)A_2L(U^n - u^n) + \sum_{j=1}^{n}\psi_j A_2(U^{n-j} - u^{n-j}) + R^n,\\
A^nE^n &\leq -\tau^\alpha\Gamma(2-\alpha)A_2LE^n + \sum_{j=1}^{n}\psi_j A_2E^{n-j} + R^n,\\
(A^n + \tau^\alpha\Gamma(2-\alpha)LA_2)E^n &\leq \sum_{j=1}^{n}\psi_j A_2E^{n-j} + R^n,
\end{aligned} \tag{4.27}$$

where $E^n = (E_1^n, E_2^n, \cdots, E_{M-1}^n)$ and $R^n = (R_1^n, R_2^n, \cdots, R_{M-1}^n)$, $1 \leq n \leq N$. Taking the inner product with E^n, on both the sides of (4.27), we have

$$\langle A^nE^n, E^n\rangle + (\tau^\alpha\Gamma(2-\alpha)L)\langle A_2E^n, E^n\rangle \leq \sum_{j=1}^{n}\psi_j\langle A_2E^{n-j}, E^n\rangle + \langle R^n, E^n\rangle. \tag{4.28}$$

For any symmetric matrix A, and any $0 \neq x \in R^{M-1}$, property of the Rayleigh–Ritz ratio is given as [108, Theorem 4.2.2],

$$\lambda_{\min}(A) \leq \frac{\langle Ax, x\rangle}{\langle x, x\rangle} \leq \lambda_{\max}(A), \tag{4.29}$$

where $\lambda_{\min}(A)$ and $\lambda_{\max}(A)$ are the minimum and maximum eigenvalues of the matrix A respectively. So we obtain,

$$\begin{aligned}
\langle A^nE^n, E^n\rangle &\geq \lambda_{\min}(A^n)\|E^n\|^2,\\
\langle A_2E^n, E^n\rangle &\geq \lambda_{\min}(A_2)\|E^n\|^2,\\
|\langle A_2E^{n-j}, E^n\rangle| \leq \langle A_2E^{n-j}, E^{n-j}\rangle^{1/2}\langle A_2E^n, E^n\rangle^{1/2} &\leq \lambda_{\max}(A_2)\|E^{n-j}\|\|E^n\|,
\end{aligned}$$

$$\langle R^n, E^n \rangle \leq \|R^n\| \|E^n\|,$$

where $\|.\|$ stands for the Euclidean norm (or l_2 norm) on R^{m-1}. From (4.28) we obtain,

$$(\lambda_{\min}(A^n) + (\tau^\alpha \Gamma(2-\alpha)L)\lambda_{\min}(A_2))\|E^n\| \leq \sum_{j=1}^{n} \psi_j \lambda_{\max}(A_2)\|E^{n-j}\| + \|R^n\|. \tag{4.30}$$

From Lemma 4.4.1 and Eq. (4.19), we see that $\lambda_{\min}(A^n) = -\psi_0$, $\lambda_{\min}(A_2) = 1$ and $\lambda_{\max}(A_2) = \frac{2}{3}$. So we have from (4.30),

$$\|E^n\| \leq \frac{1}{-\psi_0 + \tau^\alpha \Gamma(2-\alpha)L} \left[\sum_{j=1}^{n} \frac{2}{3} \psi_j \|E^{n-j}\| + \|R^n\| \right], \tag{4.31}$$

now using Gronwall's inequality [103] we obtain,

$$\begin{aligned} \|E^n\| &\leq C \frac{1}{-\psi_0 + \tau^\alpha \Gamma(2-\alpha)L} \exp\left(\frac{2}{3(-\psi_0 + \tau^\alpha \Gamma(2-\alpha)L)} \sum_{j=1}^{n} \psi_j \right) (\tau^{4-\alpha} + h^4), \\ &\leq \frac{C}{\tau^\alpha \Gamma(2-\alpha)L - 1} \exp\left(\frac{11}{9(1 - \tau^\alpha \Gamma(2-\alpha)L)} \right) (\tau^{4-\alpha} + h^4) = \tilde{C}(\tau^{4-\alpha}, h^4), \end{aligned}$$

where $\tilde{C} = \frac{C}{\tau^\alpha \Gamma(2-\alpha)L-1} \exp\left(\frac{11}{9(1-\tau^\alpha \Gamma(2-\alpha)L)}\right)$. This completes the proof. □

4.5 Numerical Experiments

In this section, we apply the discussed scheme (4.15) and (4.18) to illustrate our theoretical findings by performing numerical experiments on two test problems at the time level $T = 1$. In order to compute the errors and convergence orders in the numerical solution we use the formulas (2.40), (2.41) and (2.42). Further the error

in L_2 norm is calculated using the formula

$$\text{MAE}_2 = \max_{1\le n\le N} \sqrt{h\sum_{n=1}^{N}(U^n - u^n)^2}. \tag{4.32}$$

Example 4.5.1. Problem (4.1) reduces to fractional Fitzhugh-Nagumo (FN) reaction diffusion equation for $f(u) = u(1-u)(u-\theta)$, $0 < \theta < 1$, which is used to model the transmission of nerve impulses. We consider FN model on the domain $(x,t) \in [0, 2\pi] \times [0,1]$, with the initial and boundary conditions $u(x,0) = 0$, $u(0,t) = u(2\pi,t) = 0$, having source term $F(x,t) = t^\beta \sin\big(x/2\big)(\frac{\Gamma(\beta+1)}{\Gamma(\beta+1-\alpha)}t^{-\alpha} + (\theta + \frac{1}{4}) - (1+\theta)t^\beta \sin\big(x/2\big) + (t^\beta \sin\big(x/2\big))^2)$. Exact solution of this problem is $u(x,t) = t^\beta \sin\big(x/2\big)$, where $\beta \in \mathbb{R}^+$ such that the regularity assumption of Lemma 4.2.2 is satisfied. Here, reaction term is a nonlinear function with the Lipschitz constant 8. We compute this problem for $K = 1$, $\theta = 1/2$ and $\beta = 5$, using the proposed scheme (4.14) with tolerance $\|U^{[s+1]} - U^{[s]}\| < 10^{-8}$. In Table 4.1, we present L_∞, L_2 errors and temporal convergence order with an increasing number of partitions in the time domain and fixed spatial step size $h = 2\pi/1000$, for different values of α. From Table 4.1, we conclude the temporal convergence order is $(4-\alpha)$. Again, Table 4.2 verifies the spatial convergence order 4 for different α with fixed $\tau = 1/5000$. Fig. 4.1 gives a comparison between analytical and approximate solutions and shows that the two are well matched. Now we use following formulae to validate the convergence order graphically,

$$\epsilon(h) = \max_{0\le i\le M} \left| u_i^N(h,\tau) - u_{2i}^N\left(\frac{h}{2},\tau\right)\right|, \tag{4.33}$$

$$\epsilon(\tau) = \max_{0\le i\le M} \left| u_i^N(h,\tau) - u_i^{2N}\left(h,\frac{\tau}{2}\right)\right|. \tag{4.34}$$

For $\tau = 1/320$, the error obtained by using formula (4.33) is reported in Fig. 4.2 . It

is clear from Fig. 4.2 that the obtained numerical convergence order 4 justifies the theoretical claim. Again for $h = \frac{2\pi}{350}$ the error is plotted in Fig. 4.3 using formula (4.34) for $\alpha = 0.2, 0.4, 0.6, 0.8$. We can see from the Fig. 4.3, that slopes are 3.8, 3.6, 3.4, 3.2 respectively, which are in good agreement with the theoretical convergence order $(4 - \alpha)$. Note that, formulas (4.33) and (4.34) have been used to validate the theoretical convergence order if the exact solution is not known. Fig. 4.4 shows the behavior of the absolute error for increasing number of step sizes.

TABLE 4.1: The errors and CO for various α and fixed $h = 2\pi/1000$ for Ex. 4.5.1.

α	τ	MAE	CO	MAE_2	CO
	1/20	3.15353E-05		5.30111E-05	
	1/40	2.44496E-06	3.689083415	4.06695E-06	3.704272311
0.2	1/80	1.83879E-07	3.732982378	3.05293E-07	3.735679447
	1/160	1.37083E-08	3.745632809	2.27273E-08	3.747697361
	1/320	1.01965E-09	3.748903421	1.69190E-09	3.747709927
	1/20	1.04934E-04		1.88906E-04	
	1/40	9.17131E-06	3.516221645	1.64567E-05	3.520926652
0.4	1/80	7.81108E-07	3.553535302	1.39720E-06	3.558054181
	1/160	6.56562E-08	3.572517245	1.17395E-07	3.573097609
	1/320	5.48738E-09	3.580742947	9.80721E-09	3.581388855
	1/20	2.78565E-04		5.06914E-04	
	1/40	2.78225E-05	3.323687527	5.06152E-05	3.324099724
0.6	1/80	2.70391E-06	3.363134759	4.91548E-06	3.364166849
	1/160	2.59632E-07	3.380506368	4.71781E-07	3.381142658
	1/320	2.47804E-08	3.389201483	4.50247E-08	3.389327197
	1/20	6.73853E-04		1.20967E-03	
	1/40	7.74934E-05	3.120288473	1.39018E-04	3.121272191
0.8	1/80	8.65262E-06	3.162864056	1.55206E-05	3.163020464
	1/160	9.53561E-07	3.181740149	1.71041E-06	3.181775839
	1/320	1.04430E-07	3.190778844	1.87316E-07	3.190792424

TABLE 4.2: The errors and CO for various α and fixed $\tau = 1/5000$ for Ex. 4.5.1.

α	h	MAE	CO	MAE_2	CO
0.2	1/4	2.16332E-04		4.17084E-04	
	1/8	1.33507E-05	4.018254217	3.57860E-05	3.542869421
	1/16	8.30850E-07	4.006190465	3.14701E-06	3.507339423
	1/32	5.18464E-08	4.002270780	2.77683E-07	3.502470078
	1/64	3.22971E-09	4.004765922	2.43262E-08	3.512858413
	1/128	2.92480E-10	3.464996153	1.85174E-09	3.715554308
0.4	1/4	1.70069E-04		3.19104E-04	
	1/8	1.04874E-05	4.019389979	2.75256E-05	3.535181590
	1/16	6.49723E-07	4.012690737	2.41042E-06	3.513417607
	1/32	3.76455E-08	4.109274451	1.97506E-07	3.609308823
	1/64	2.25568E-09	4.060844335	1.67281E-08	3.561549767
	1/128	1.32657E-10	4.087784302	1.21030E-09	3.788834631
0.6	1/4	1.27597E-04		2.33887E-04	
	1/8	7.85525E-06	4.021797274	2.02389E-05	3.530607657
	1/16	4.85838E-07	4.015109657	1.76974E-06	3.515526892
	1/32	2.73694E-08	4.149837040	1.40992E-07	3.649844620
	1/64	1.53980E-09	4.151748516	9.10904E-09	3.952178268
	1/128	8.49025E-11	4.180796108	5.38218E-10	4.081035897
0.8	1/4	9.24643E-05		1.66775E-04	
	1/8	5.68781E-06	4.022952268	1.44630E-05	3.527465050
	1/16	3.54406E-07	4.004395842	1.27427E-06	3.504618073
	1/32	2.26245E-08	3.969449562	9.34425E-08	3.769458337
	1/64	1.44969E-09	3.964063382	5.58681E-09	4.063980251
	1/128	1.17246E-10	3.628136943	3.19540E-10	4.127956047

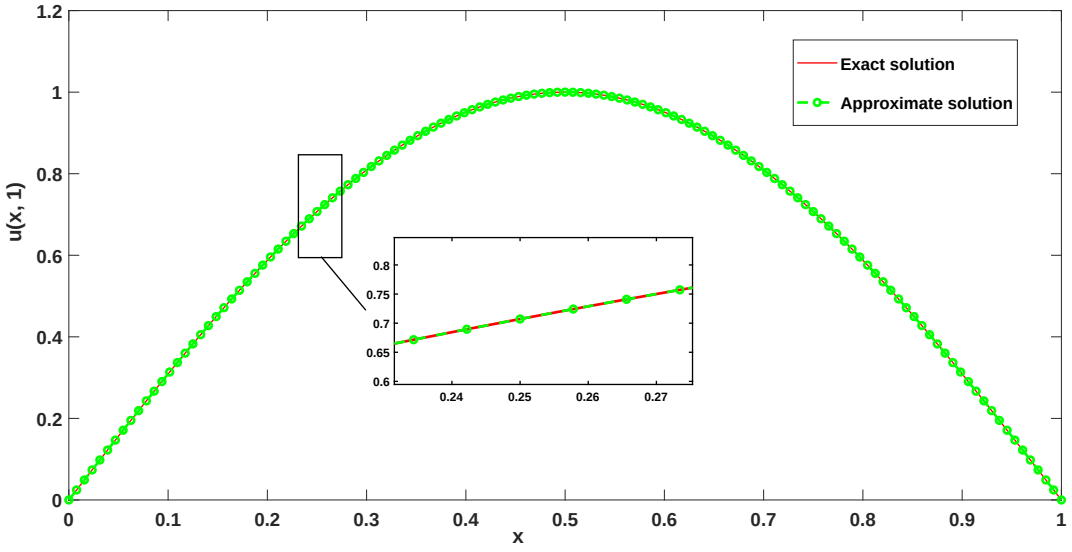

FIGURE 4.1: Graph of exact and approximate solutions obtained for $\alpha = 0.25$, $h = 1/128$ and $\tau = 1/50$ for Ex. 4.5.1.

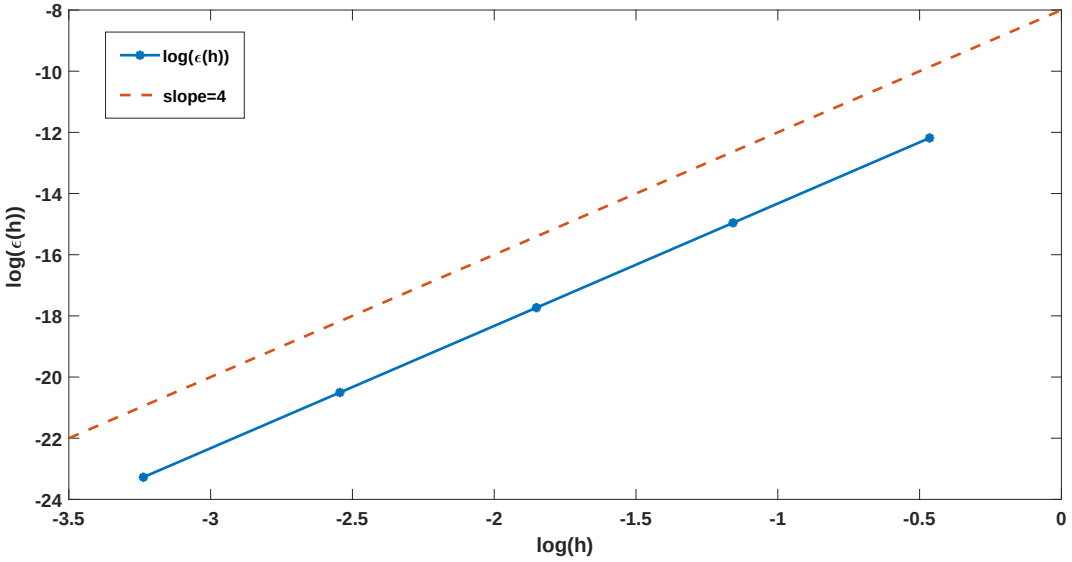

FIGURE 4.2: Convergence order in spatial direction for $\alpha = 0.2$ for Ex. 4.5.1.

Example 4.5.2. [109] Consider the time fractional generalized Fisher's reaction–diffusion equation,

$$ {}_0^C D_t^\alpha u(x,t) - u_{xx} - u(x,t)(1-u^2(x,t)) = F(x,t), (x,t) \in [0,1] \times [0,1], $$

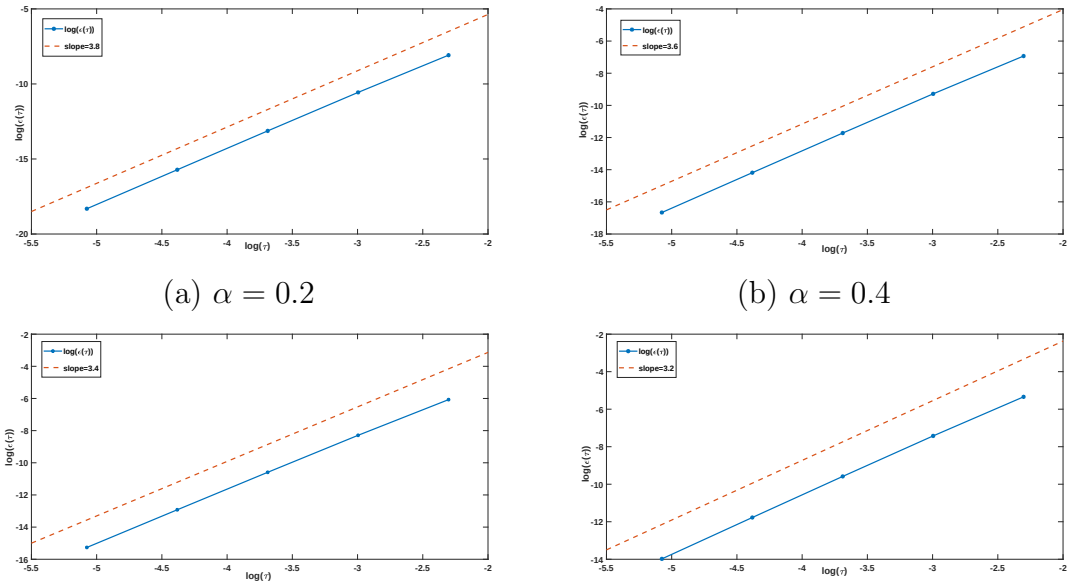

(a) $\alpha = 0.2$ (b) $\alpha = 0.4$

(c) $\alpha = 0.6$ (d) $\alpha = 0.8$

FIGURE 4.3: Convergence orders in temporal direction for $\alpha = 0.2,\ 0.4,\ 0.6,\ 0.8$ for Ex. 4.5.1.

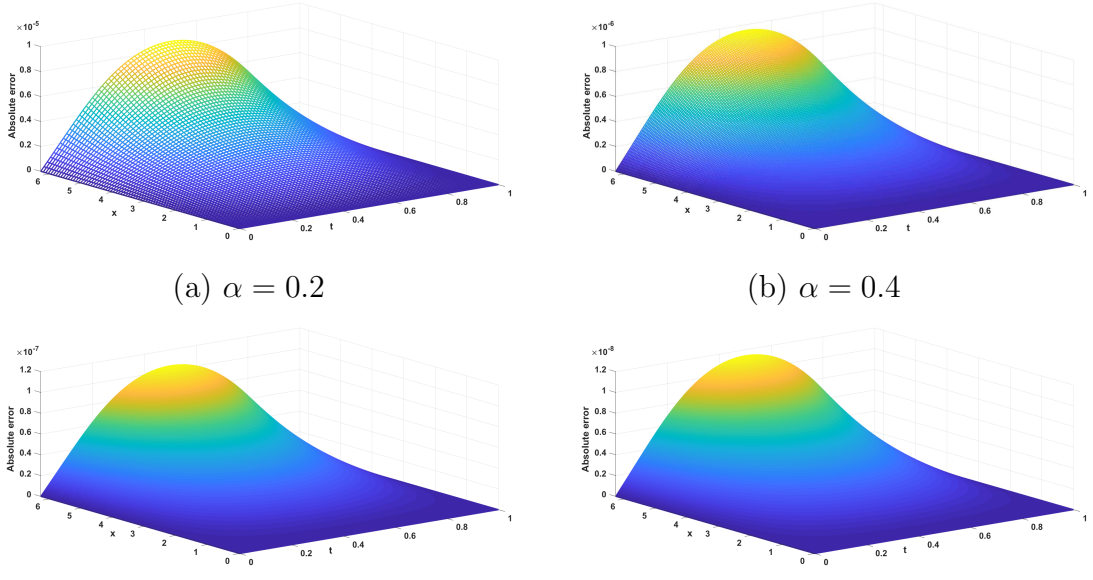

(a) $\alpha = 0.2$ (b) $\alpha = 0.4$

(c) $\alpha = 0.6$ (d) $\alpha = 0.8$

FIGURE 4.4: Absolute error plot for different step sizes with $\alpha = 0.8$ for Ex. 4.5.1.

with the initial and boundary conditions, $u(x,0) = 0$, and $u(0,t) = u(1,t) = 0$. The source term is given as, $F(x,t) = \frac{24t^{4-\alpha}}{\Gamma(5-\alpha)}\sin(2\pi x) + (4\pi^2 - 1)t^4\sin(2\pi x) + (t^4\sin(2\pi x))^3$, with exact solution $u(x,t) = t^4\sin(2\pi x)$. For this equation, $f(u) = u(1-u^2)$, which is a nonlinear function of u with Lipschitz constant 4. The L_∞, L_2 errors and convergence order are computed in the spatial and the temporal direction using the difference scheme (4.18) s.t. $\|U^{[s+1]} - U^{[s]}\| < 10^{-8}$. Numerical results are shown through Table 4.3 and Table 4.4 which validate the theoretical findings. A comparative analysis of the numerical and the analytical solutions can be seen from Fig. 4.5. Using formulas (4.33) and (4.34) we validate the theoretically established temporal and spatial convergence orders. Fig. 4.6 verifies the theoretically claimed spatial convergence order 4. From Fig. 4.7, we see that the slopes agree well for various α with the theoretical result of $4-\alpha$. Fig. 4.8 gives a comparison between absolute errors for increasing step sizes $h = \tau = 1/80, 1/160, 1/320, 1/640$.

TABLE 4.3: The errors and CO for various values of α and fixed $h = 1/1000$ for Ex. 4.5.2.

α	τ	MAE	CO	MAE_2	CO
	1/10	8.78396E-06		6.22426E-06	
	1/20	1.03893E-06	3.079769295	7.36181E-07	3.079769496
0.2	1/40	9.73670E-08	3.415525444	6.87938E-08	3.419711076
	1/80	8.37465E-09	3.539333064	5.88184E-09	3.547938333
	1/160	6.89163E-10	3.603111257	4.81851E-10	3.609607096
	1/10	2.05941E-05		1.45927E-05	
	1/20	2.43033E-06	3.083008750	1.72198E-06	3.083110472
0.4	1/40	2.42479E-07	3.325219114	1.70256E-07	3.338293511
	1/80	2.25755E-08	3.425030122	1.57197E-08	3.437057853
	1/160	2.02844E-09	3.476313537	1.40449E-09	3.484452416
	1/10	4.07006E-05		2.77365E-05	
	1/20	4.61702E-06	3.140016848	3.24593E-06	3.095081443
0.6	1/40	4.92170E-07	3.229735278	3.42019E-07	3.246485418
	1/80	5.02305E-08	3.292520947	3.46148E-08	3.304613771
	1/160	5.01661E-09	3.323779490	3.43898E-09	3.331336966
	1/10	9.68575E-05		5.26174E-05	
	1/20	9.55392E-06	3.341699470	6.22732E-06	3.078856507
0.8	1/40	1.03424E-06	3.207510689	7.08939E-07	3.134877972
	1/80	1.16715E-07	3.147509157	7.95618E-08	3.155512714
	1/160	1.30464E-08	3.161274814	8.86379E-09	3.166081608

TABLE 4.4: The errors and CO for various α and fixed $\tau = 1/5000$ for Ex. 4.5.2.

α	h	MAE	CO	MAE_2	CO
0.2	1/4	2.57991E-02		1.82427E-02	
	1/8	1.52151E-03	4.083736522	1.52523E-03	3.580212992
	1/16	9.33900E-05	4.026098273	1.32353E-04	3.526564937
	1/32	5.81020E-06	4.006608817	1.16448E-05	3.506633024
	1/64	3.62695E-07	4.001759886	1.02801E-06	3.501761359
	1/128	2.26354E-08	4.002101166	9.07322E-08	3.502101281
0.4	1/4	2.55516E-02		1.80676E-02	
	1/8	1.50653E-03	4.084106821	1.51020E-03	3.580595336
	1/16	9.24710E-05	4.026088571	1.31050E-04	3.526552252
	1/32	5.75284E-06	4.006655443	1.15298E-05	3.506679505
	1/64	3.58925E-07	4.002519726	1.01732E-06	3.502521164
	1/128	2.22109E-08	4.014340769	8.90300E-08	3.514341027
0.6	1/4	2.52509E-02		1.78550E-02	
	1/8	1.48813E-03	4.084764645	1.49173E-03	3.581272571
	1/16	9.13419E-05	4.026077856	1.29448E-04	3.526536765
	1/32	5.68242E-06	4.006699963	1.13885E-05	3.506723793
	1/64	3.54353E-07	4.003247519	1.00435E-06	3.503248940
	1/128	2.17491E-08	4.026158220	8.71779E-08	3.526158245
0.8	1/4	2.48906E-02		1.76002E-02	
	1/8	1.46580E-03	4.085837163	1.46932E-03	3.582376209
	1/16	8.99728E-05	4.026057092	1.27506E-04	3.526508417
	1/32	5.59768E-06	4.006588157	1.12185E-05	3.506611619
	1/64	3.49498E-07	4.001471032	9.90578E-07	3.501472454
	1/128	2.18816E-08	3.997490749	8.77080E-08	3.497490734

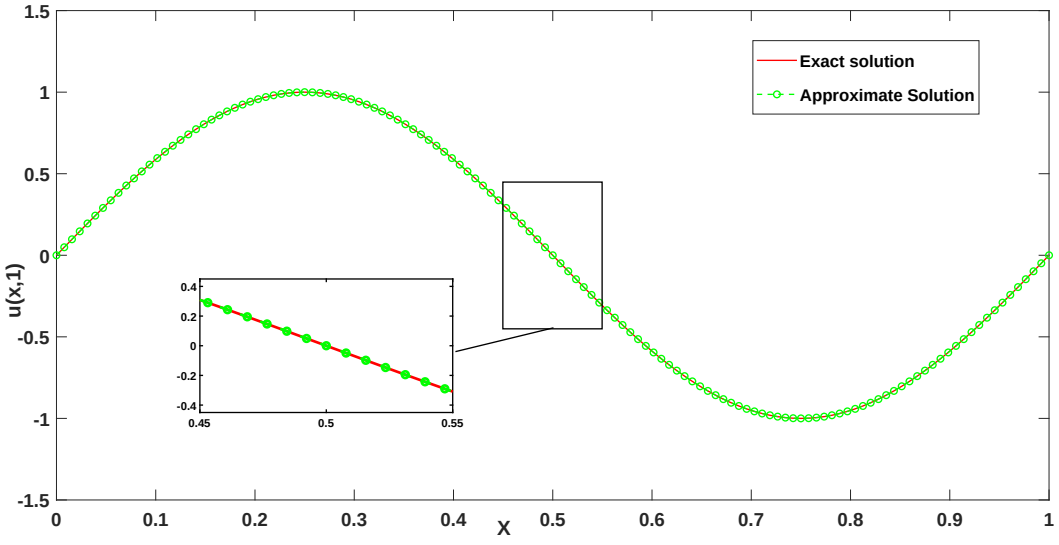

FIGURE 4.5: Graph of exact and approximate solutions obtained for $\alpha = 0.25$, $h = 1/128$ and $\tau = 1/50$ for Ex. 4.5.2.

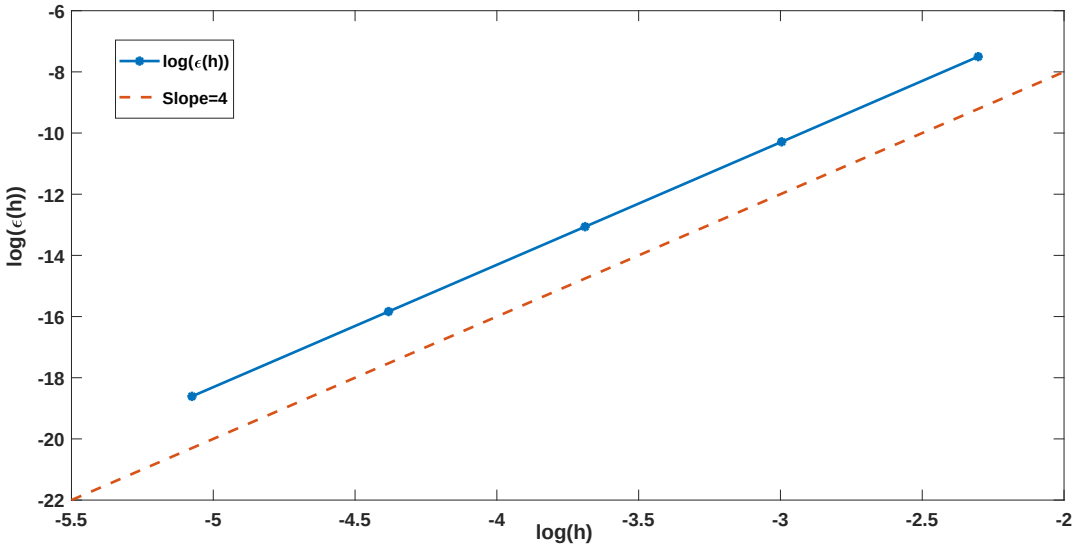

FIGURE 4.6: Convergence order in spatial direction for $\alpha = 0.2$ for Ex. 4.5.2.

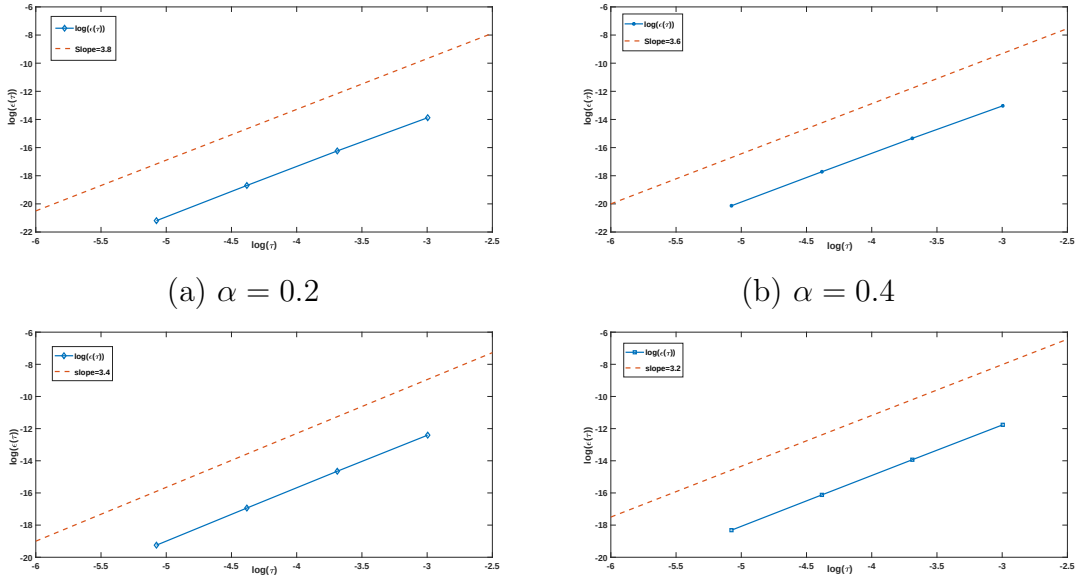

(a) $\alpha = 0.2$ (b) $\alpha = 0.4$

(c) $\alpha = 0.6$ (d) $\alpha = 0.8$

FIGURE 4.7: Convergence orders in temporal direction for $\alpha = 0.2,\ 0.4,\ 0.6,\ 0.8$ for Ex. 4.5.2.

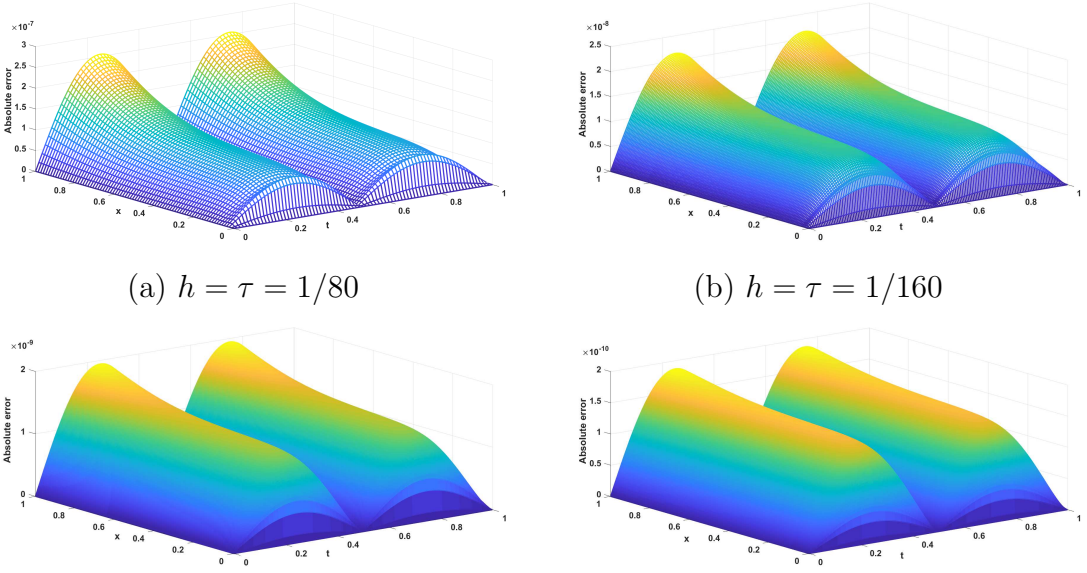

(a) $h = \tau = 1/80$ (b) $h = \tau = 1/160$

(c) $h = \tau = 1/320$ (d) $h = \tau = 1/640$

FIGURE 4.8: Absolute error plot for different step sizes with $\alpha = 0.8$ for Ex. 4.5.2.

4.6 Conclusions

A time stepping cubic approximation scheme for a time fractional nonlinear reaction–diffusion equation is described and demonstrated. Further, it is combined with a 4th order compact difference scheme for space discretization. Together with these additions, the Newton's approach for handling the nonlinear system improves the convergence order in the temporal direction compared to the existing works in the literature. Stability and convergence analysis of the numerical method are studied rigorously using von Neumann analysis and matrix analysis, respectively. Simulation results obtained from the test examples confirm the sharpness of the achieved convergence rates in the time-space directions.

****